



Surface enriched palladium on palladium-copper bimetallic nanoparticles as catalyst for polycyclic triazoles synthesis

Rajib Saha, Dhanarajan Arunprasath, Govindasamy Sekar*

Department of Chemistry, Indian Institute of Technology Madras, Chennai, Tamil Nadu 600036, India

ARTICLE INFO

Article history:

Received 11 March 2019
Revised 23 July 2019
Accepted 31 July 2019
Available online 27 August 2019

Dedicated to Prof. P. Selvam on the occasion of his 60th birthday.

Keywords:

Bimetallic nanoparticles
Palladium
Copper
Nano catalysis
Polycyclic triazoles
C–H functionalization

ABSTRACT

Transition-metal nanoparticles (NPs) gained interest as a catalyst due to their high reactivity and recyclability. Monometallic NPs are less catalytic active compared to homogeneous counterparts as less number of catalytic active metal atoms are present on the surface of NPs and metal atoms present in the core part of the NPs are not utilized. It is necessary to synthesize a stable, reusable, highly reactive and economic catalyst which contain a more number of catalytic active precious metal atoms on the surface of NPs. Here in we have synthesized metal-carbon bond stabilized, alloy structured Pd/Cu bimetallic nanoparticles using binaphthyl moiety as a stabilizer (Pd/Cu-BNP). The enrichment of catalytically active precious Pd atoms over inexpensive Cu on the surface was observed with a narrow size distribution of the nanoparticles (average diameter 3 ± 0.5 nm). The Pd/Cu-BNP was used as an efficient and recyclable catalyst for the synthesis of polycyclic triazoles through domino alkyne insertion and C–H bond functionalization reaction sequence.

© 2019 Published by Elsevier Inc.

1. Introduction

Transition-metal based nanoparticles have received much attention recently due to their great potential in catalyzing various types of organic transformations as well as being stable and reusable than traditional homogenous metal catalysts [1,2]. However, most of the highly stable transition metal nanoparticles have not been used as catalysts for organic synthesis as they are less reactive. In this context, recently our research group reported a Pd-C_(binaphthyl) covalent bond stabilized palladium nanocatalyst (Pd-BNP) with a narrow size distribution which generally shown efficient catalytic activity in annulation, C–H activation, reductive Heck, reduction, and cross-coupling reactions [3–8]. The catalyst was prepared by grafting binaphthyl moiety over Pd during the reduction of K₂PdCl₄ using NaBH₄ in toluene as solvent.

In general, monometallic NPs are less catalytic active than its homogeneous counterparts due to surface phenomenon, i.e. active metal component present on the surface of NPs could only catalyze the reaction [9]. The straightforward approach to improve the catalytic properties of monometallic NPs is to include a second metal to enrich the density of active sites on the surface of the catalysts. The presence of hetero metal-metal interactions could induce the

beneficial synergistic effect between the electronic and geometric properties which attributes its unique enhanced selectivity, reactivity and stability of the bimetallic nanoparticles (BMNPs) [10–16]. Moreover, these BMNPs are known to have better stability, robustness and less susceptibility to aggregation and deactivation during the catalytic process compared to the corresponding monometallic counterparts. The continuous research in this field has led to the development of several BMNPs having specific morphologies such as random alloy, core-shell and porous structure [17–25]. For example, a bimetallic Rh/Fe nanoparticles stabilized by phenylazomethine dendrimers (TPP-DPA G4) was elegantly synthesized and utilized for hydrogenation of olefins and nitroarenes [26].

The concept of covalent stabilization of nanoparticles was recently pioneered by Mirkhalaf and co-workers for Au and Ag monometallic NPs [27]. However, the synthesis of BMNPs stabilized by metal-carbon covalent bonds has not been attempted so far. We questioned whether it could be possible to apply our monometallic Pd-BNP synthesis strategy to achieve BMNPs. Being non-toxic, cost-effective and environmentally benign, copper drew our attention to be chosen as a second component to prepare the economic BMNPs. Herein, we describe the synthesis of surface enriched Pd on Pd/Cu-BNP which are stabilized by the simple and effective binaphthyl moiety and its applications in the synthesis of densely substituted tricyclic triazoles under mild reaction conditions.

* Corresponding author.

E-mail address: gsekar@iitm.ac.in (G. Sekar).

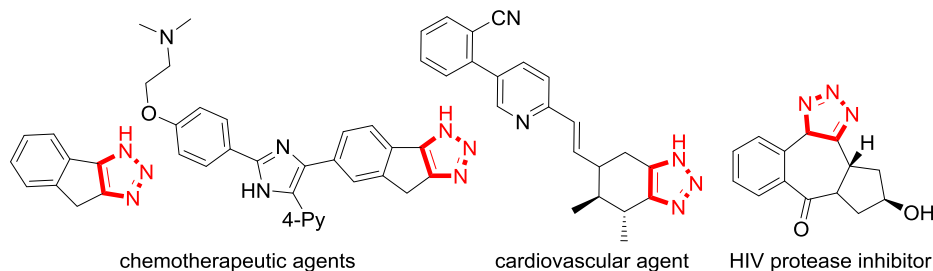


Fig. 1. Examples of biologically important fused 1,2,3-triazoles.

1,2,3-Triazoles are important nitrogen containing heterocyclic motifs due to its rich and intriguing biological and physical properties. Specifically, compounds containing fused triazoles have become a key structural core of potential pharmacological substances such as chemotherapeutic and cardiovascular drugs [28–31]. Some of the biologically active molecules containing fused 1,2,3-triazole ring are shown in Fig. 1. For these reasons, more efforts have been devoted to develop different methods to synthesize fused triazoles [32,33]. Lautens research group recently reported synthesis of fused triazole through multi-component strategy using Herrmann-Beller palladacycle precatalyst [34]. Despite of all the advances made to synthesize fused triazoles, still efforts are required to develop more sustainable, milder, yet environment-friendly approach to construct poly functionalized triazoles.

2. Results and discussion

2.1. Synthesis of bimetallic nanocatalysts

The preparation of Pd/Cu-BNP involves two step process following our procedure for the monometallic Pd NPs as shown in Scheme 1. Initially, 2,2'-binaphthalene-bisdiazonium tetrafluoroborate was prepared from the 1,1'-binaphthyl-2,2'-diamine (BINAM) using HBF_4 and NaNO_2 at 0 °C. Then, simultaneous reduction of $\text{Pd}(\text{OAc})_2$ and $\text{Cu}(\text{OAc})_2$ (1:1) using NaBH_4 was carried out in the presence of diazonium salt. The heat generated from the reduction leads to the generation of binaphthyl radical which stabilizes the nanoparticles via a strong Pd–C [3,27,35] and Cu–C covalent bond linkages. The resulting Pd/Cu-BNP was found to be highly stable under air and no physical changes occurred over time.

2.2. Characterization of synthesized Pd/Cu bimetallic nanocatalysts

The newly developed Pd/Cu-BNP was characterized using IR, ^1H NMR, ^{13}C NMR, TEM, ICP, TGA, powder XRD and XPS analyses (See SI for more details).

The comparison of FTIR spectra of the corresponding BINAM diazonium salt and Pd/Cu-binaphthyl NPs, the absence of absorption band at 2260 cm^{-1} in the Pd/Cu-BNPs revealed that the NPs

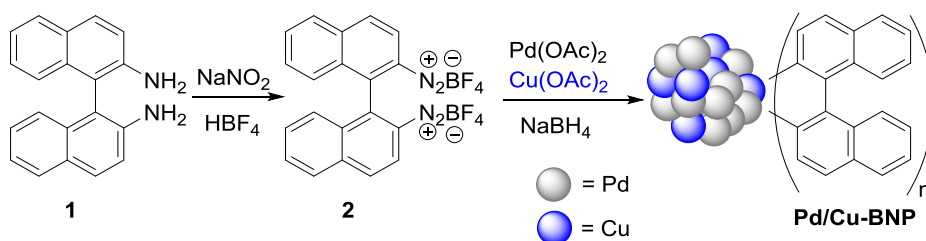
are free from the diazonium salt (Fig. 2a). The peaks at 3050 cm^{-1} and 2929 cm^{-1} in Pd/Cu NPs are due to the stretching vibrations of aromatic C–H bond. The peaks at 1130, 812, 745 and 626 cm^{-1} are due to C–H bending and peaks at 1609 and 1500 cm^{-1} are due to C=C vibrations, all of which confirmed the presence of the binaphthyl moiety in the Pd/Cu NPs. The characteristic peaks of CuO at 536 and 482 cm^{-1} are absent in synthesized Pd/Cu nanoparticles which implies that NPs is free from CuO. Further, the presence of Pd–C covalent bond in Pd/Cu-BNP was confirmed, as the peak presence at 545 cm^{-1} which is known as characteristic peak for C(sp²)-Pd bond stretching vibration [36] (Fig. 2b).

In the ^1H NMR, broad multiplet peaks were observed at 6.29–8.30 ppm corresponds to aromatic C–H (Fig. 2c). In solid state ^{13}C NMR, a broad peak was found at 110–145 ppm which are corresponds to aromatic sp² carbons (Fig. 2d). The both ^1H NMR and solid state ^{13}C NMR results confirmed that the aromatic binaphthyl moiety is present in Pd/Cu-BNPs nanoparticles.

The parallel beam X-ray diffraction was used to further confirm the crystalline nature of Pd/Cu-BNP. Fig. 3 showed the Bragg diffraction of Pd/Cu-BNP and broad peaks were observed due to small particle size (2–5 nm). Distinct peaks were observed at 40.3, 47.1 and 69.0 which might be corresponded to the Pd (1 1 1), Pd(2 0 0) and Pd(2 2 0) crystal planes respectively (Fig. 3, top). No credible peak was observed for the Cu in Pd/Cu-BNP which illustrates that the surface is enriched with Pd atoms. The bimetallic Pd/Cu-BNP showed a slight deviation of peak from monometallic Pd-BNP due to the less atomic radius of Cu than Pd. Further, using the Debye-Scherrer equation the particle size of Pd/Cu-BNP was calculated and found the average particle size is 3.8 nm (see SI, Fig. S7).

The high resolution TEM images of Pd/Cu-BNP (Fig. 4a) showed that most of the particles are spherical in shape and well dispersed without any apparent aggregation. The average size distribution of Pd/Cu-BNP is $3.00 \pm 0.5\text{ nm}$ (Fig. 4b). A well-defined lattice fringe of 0.22 nm was seen which is ascribed to the Pd/Cu (1 1 1) lattice plane (c and d).

The high angle annular dark-field scanning transmission electron microscopy (HAADF-STEM) equipped with energy dispersive X-ray (EDX) elemental mapping analysis was used to examine the micro structure, elemental distribution and the interaction of



Scheme 1. Synthesis of Pd/Cu-BNP.

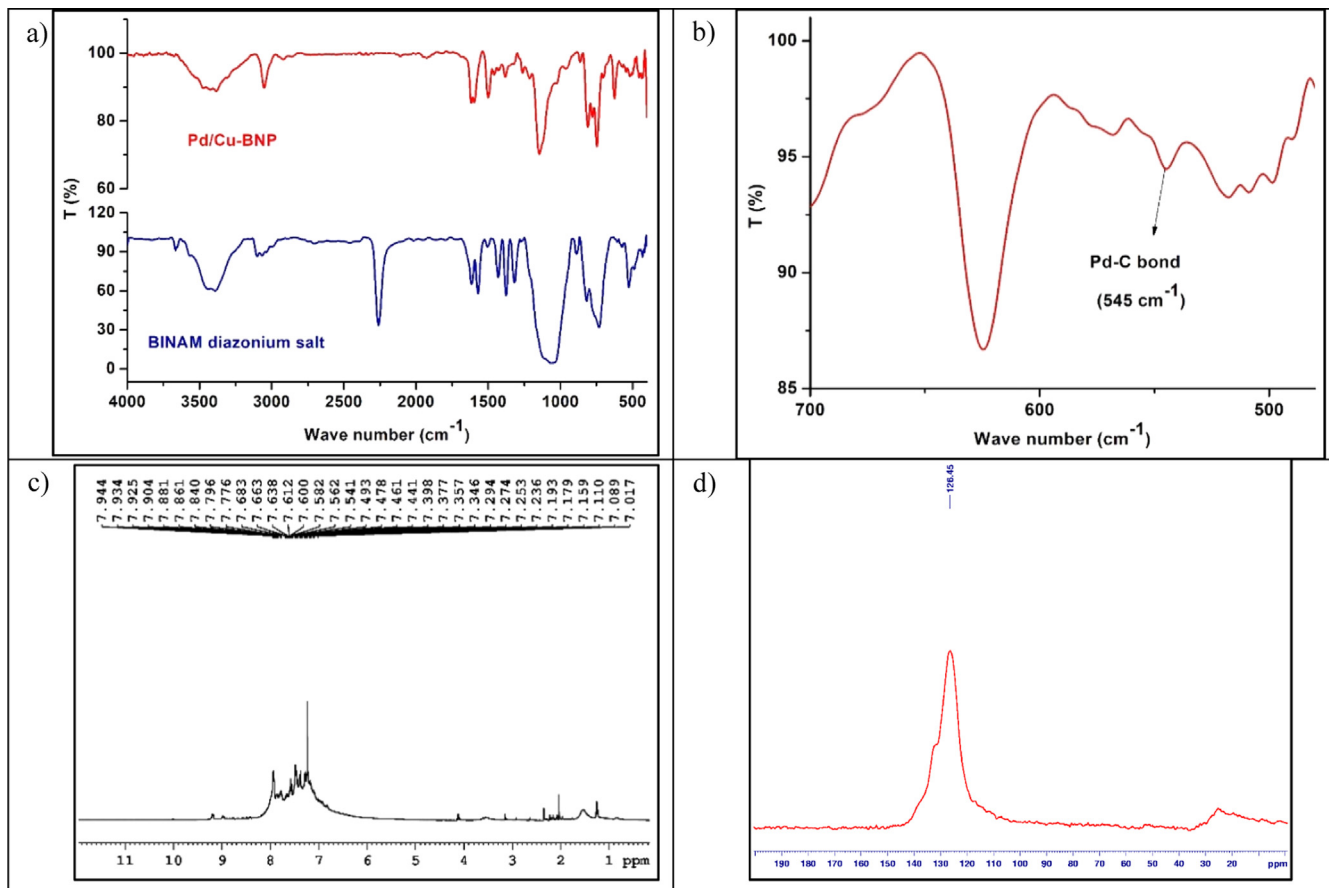


Fig. 2. Selected characterizations of Pd/Cu-BNP. (a and b) FTIR spectra of Pd/Cu-BNP (c and d) ¹H NMR and solid state ¹³C NMR of Pd/Cu-BNP.

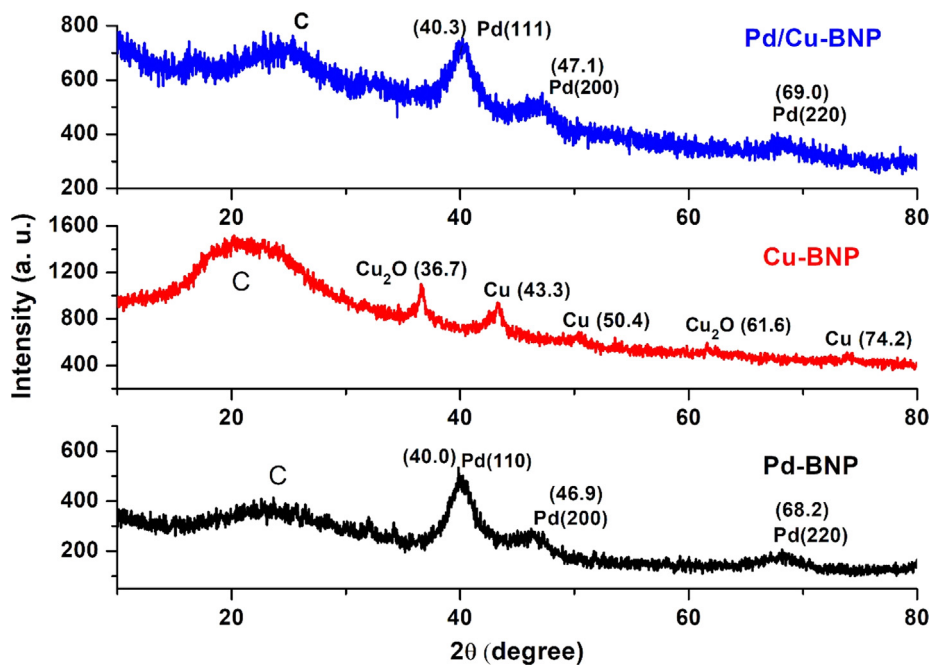


Fig. 3. Powder XRD patterns of Pd-BNP (bottom), Cu-BNP (middle), Pd/Cu-BNP (top).

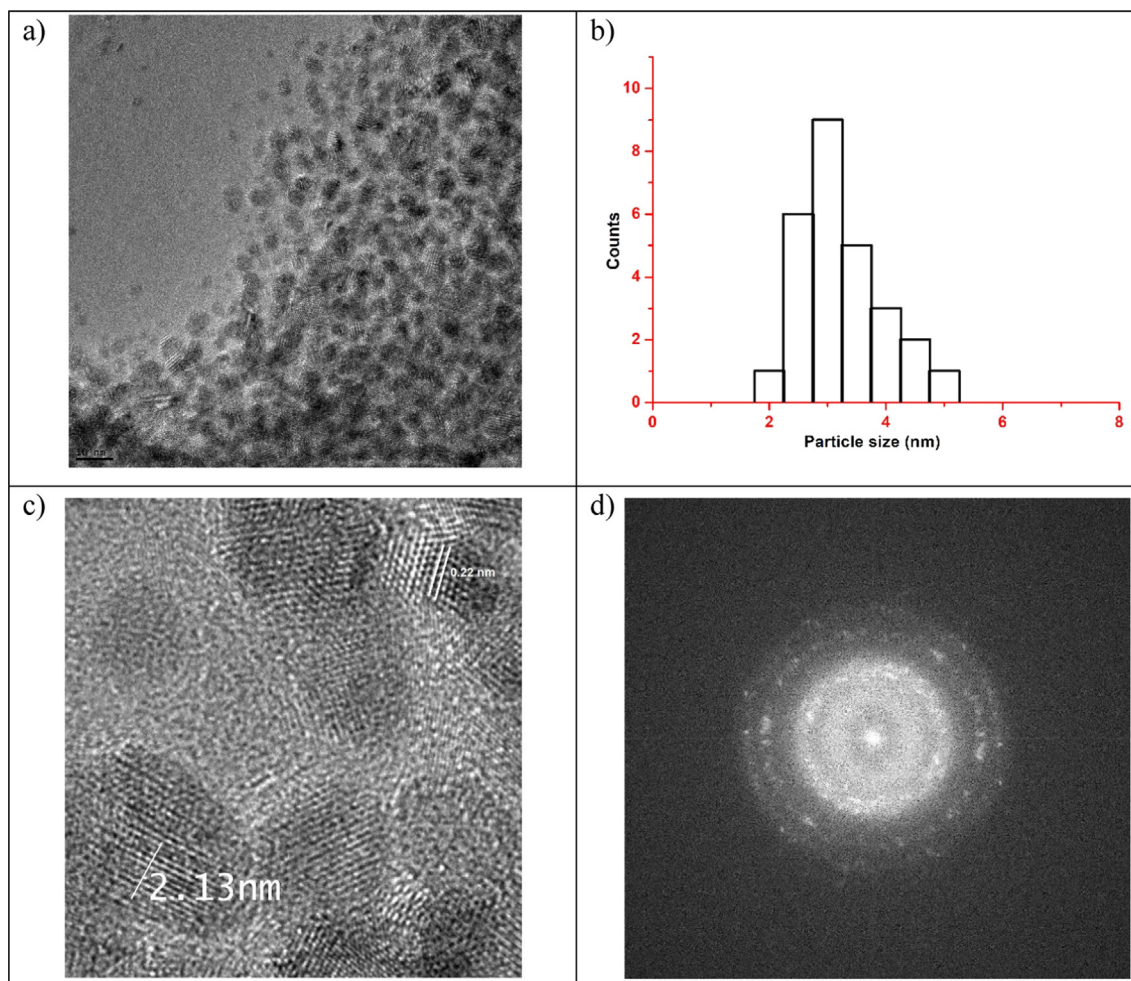


Fig. 4. (a) HRTEM images of Pd/Cu-BNP, (b) Histogram of particles size distribution of Pd/Cu-BNP (c) well-defined lattice fringe of 0.22 nm for Pd/Cu-BNP, (d) SEAD image of Pd/Cu-BNP.

the metal to BNP of the synthesized nanoparticles (Fig. 1). The coloured elemental mapping images showed that palladium atoms (green, Fig. 5c), copper atoms (blue, Fig. 5d) and carbon atoms (cyan, Fig. 5e) were uniformly distributed with a characteristic alloy structure. This analysis indicated the presence of Pd, Cu and C in the same nanoparticle. It can also be observed in overlay image that, a very thin shell of Pd was noted on the surface which confirms the surface enrichment of the Pd atoms in the Pd/Cu-BNP (Fig. 5f, also see SI and Fig. S4). Further, palladium enrich surface was confirmed from the EDX line profile shown in Fig. 5g, h and i. Both, the elemental mapping and the EDX line profile were confirmed that the palladium surface enrich Pd/Cu alloy nanoparticles is surrounded by binaphthyl moiety.

The XPS pattern of Pd/Cu-BNP showed that the binding energy of most of the palladium species shifted towards higher binding energy region (Pd 3d_{5/2} at 337.35) and for copper shifted towards lower binding energy region (Cu 2p_{3/2} at 928.36) (Fig. 6). The abnormal shift in binding energy could be explained as the metallic bonded (Pd–Cu) electron shifted from palladium to copper in Pd/Cu bimetallic NPs because Cu has higher electron affinity (1.24 eV) compared to the Pd (0.56 eV). As a results, electron deficient Pd showed higher binding energy and electron rich Cu showed lower binding energy. In literature, this type of binding energy shift is observed some other nano alloy type nanoparticles such as Pt/Co, Pt/Ru, Pd/Ag and Pd/Cu [37–39].

The next attention was turned towards testing the catalytic performance of the Pd/Cu-BNP in domino synthesis of triazoles via carbometalation and C–H functionalization. It must be noted that the catalytic activity investigation of most of the developed BMNPs are restricted to simple hydrogenation reactions of nitroarenes and olefins [40–42]. The usage of BMNPs in domino reactions which involves multiple bond formation in a single step has never been investigated.

2.3. Investigations of reaction conditions and scope

Our effort to synthesize polycyclic triazoles through sustainable manner began by choosing triazole-bearing aryl iodide (**3a**) and diphenylacetylene (**4a**) as model substrates. The initial reaction was carried out in the presence of 2.5 mol% Pd/Cu-BNP (10 wt% Pd and 5 wt% of Cu by ICP-OES analysis) and 3 equiv. of Et₃N in DMF as solvent. The Pd/Cu-BNP has shown excellent catalytic activity as the desired product via domino carbopalladation and C(sp²)-H functionalization was isolated in 79% yield (Table 1, entry 1).

Then, different metal NPs were screened, concentrating impact of their catalytic activity. The other bimetallic Pd/Cu-QNP and Pd/Cu-PNP provided 74% and 67% yield of **5a**. Our monometallic Pd-BNP furnished the product in 65% yield (entry 6). Cu-BNP was unable to give **5a** (entry 4). Notably, the mixture of Pd-BNP and

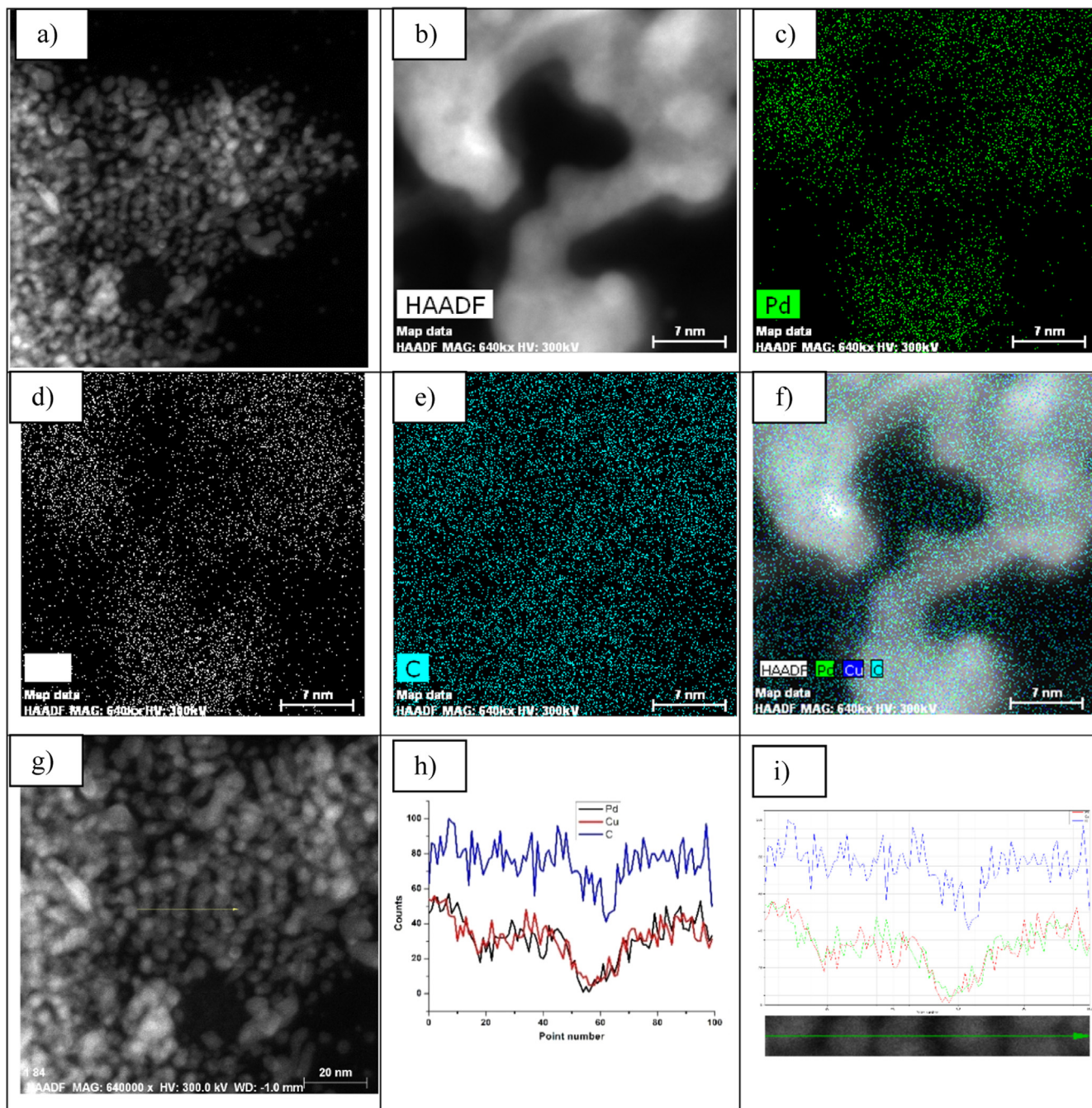


Fig. 5. Selected Characterizations of Pd/Cu-BNP. (a and b) HAADF of Pd/Cu-BNP, STEM-EDX elemental mapping of HRTEM image, (c) Pd, (d) Cu, (e) C (f) Pd/Cu-BNP (overlay), Line mapping (g) HAADF, (h) The line profile of Pd, Cu and C (i) Line profile along with particles.

Cu-BNP (1:1) has also shown less catalytic activity (67%, entry 5). Other catalysts such as Pd-PNP, Pd-QNP and commercial NPs furnished the product in 53–66% yields (entries 7–9). Screening of various catalysts manifested that bimetallic Pd/Cu-BNP is more effective for the present transformation than other catalysts due to the presence of more number of active metal components (Pd) on the surface which increases the efficiency.

To further improve the yield of tricyclic triazole **5a**, other parameters were screened and results are summarized in Table 2. The other bases including organic bases (DBU and DIPEA) and inorganic bases (KF and K_2CO_3) were found less efficient than Et_3N for the current transformation (entries 1–4).

Then the effect of solvent was investigated. Polar aprotic solvents such as DMSO and DMA afforded the desired product in 62% and 50% yields respectively (entries 5 and 6). Interestingly, the reaction occurred in water medium albeit with poor yield (20%, entry 7). The reaction temperature influenced the reaction outcome as decreasing the reaction temperature to 110 °C led to an increase in the yield to 81% (entry 10). In absence of base reaction did not provide any yield of product **5a** (entry 11). This results implies that the reaction catalyzed by base can be rule out and Pd/Cu-BNP is crucial for these methodology. The changes in catalyst loading did not help to increase the yield (entries 12 and 13). Surprisingly, the maximum yield of 93% was observed when the

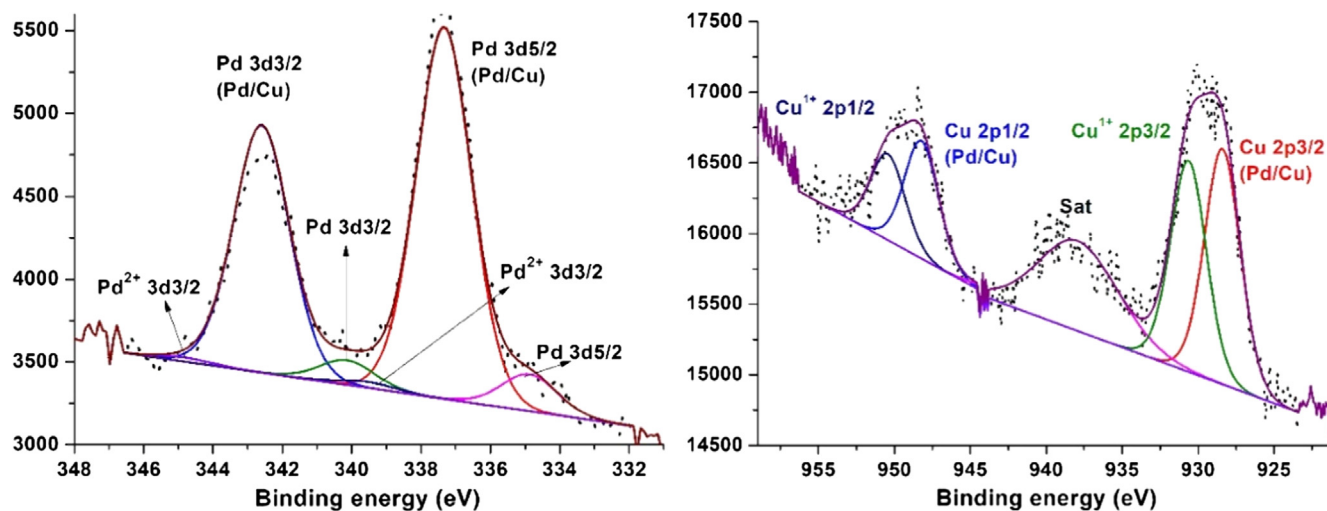


Fig. 6. XPS pattern of Pd/Cu-BNP for Pd (left) and Cu (right).

Table 1
Screening of different metal NPs.^a

Entry	Cat.	Yield (%)	Entry	Cat.	Yield (%)
1	Pd/Cu-BNP ⁿ	79	6	Pd-BNP ⁿ	65
2	Pd/Cu-QNP ⁿ	74	7	Pd-PNP ⁿ	62
3	Pd/Cu-PNP ⁿ	67	8	Pd-QNP ⁿ	63
4	Cu-BNP ⁿ	00	9	Commercial Pd-NP (20-30 nm)	66
5	Pd-BNP : Cu-BNP (1:1)	67	10	Pd/C	53

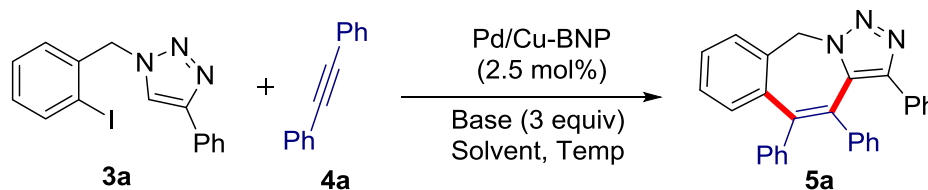
^a All the reactions were carried out on 0.25 mmol scale and isolated yields are shown.

reaction was carried out in presence of 50 mol% AcOH presumably due to assistance of carboxylate ligand in the C–H activation (entry 14). Further changing the amount of AcOH did not improve the yield (entries 15 and 16).

With the optimized reaction conditions in hand, the substrate scope for this domino reaction was surveyed (Table 3). The reac-

tion conditions were tolerant with electron-donating and electron-withdrawing substituents, as in all the cases the desired products were isolated in good to excellent yields. At first, triazoles with electron-donating groups such as 4-Me, 4-pentyl, 4-OMe and 3-Me were employed with **4a** and the desired products were obtained in 84–91% yields (**5b–e**). Triazoles with aliphatic

Table 2
Optimization of the reaction conditions.



Entry	Base	Solvent	Temp. (°C)	Yield (%) ^{a,b}
1	DBU	DMF	120	8
2	DIPEA	DMF	120	52
3	KF	DMF	120	60
4	K ₂ CO ₃	DMF	120	9
5	Et ₃ N	DMSO	120	62
6	Et ₃ N	DMA	120	50
7	Et ₃ N	H ₂ O	120	20
8	Et ₃ N	THF	120	00
9	Et ₃ N	DMF	130	55
10	Et ₃ N	DMF	110	81
11	–	DMF	110	00
12 ^c	Et ₃ N	DMF	110	66
13 ^d	Et ₃ N	DMF	110	72
14 ^e	Et ₃ N	DMF	110	93
15 ^f	Et ₃ N	DMF	110	86
16 ^g	Et ₃ N	DMF	110	90

^a Reaction conditions: **3a** (0.25 mmol) and **4a** (0.375 mmol).

^b Isolated yields are shown.

^c 1.5 mol% of Pd/Cu-BNP.

^d 3.0 mol% of Pd/Cu-BNP.

^e 50 mol% AcOH was used.

^f 25 mol% of AcOH was used.

^g 1.0 equiv. of AcOH was used.

side-chains such as *n*-butyl, *t*-butyl and cyclopropyl were found to be suitable substrates as the corresponding products (**5f–h**) were isolated in 84%, 80% and 82% yields respectively.

Next the scope of this transformation was explored with various substituted diarylacetylenes. 4-Me and 4-OMe substituted diphenylacetylenes afforded the corresponding products **5i** and **5j** in 84% and 85% yields respectively. Electron-withdrawing substituents such as F, CF₃, CO₂Et and CN were found to be compatible as the products **5k–o** were isolated in 68–90% yields. 2-Thienyl attached acetylene was also found to be reactive under the optimized reaction conditions and gave yield of corresponding product **5p** in 77%. The substrates containing divergent substituents were also efficiently converted into the annulated tricyclic triazoles in good yields (**5q–w**, 75–88%). However, 2-pyridine attached triazole and aliphatic acetylene did not provide the desired product under the optimized reaction conditions. The unsymmetrical diarylacetylene (1-methoxy-4-(phenylethynyl)benzene) gave inseparable mixture of two regioisomer ratio in 1:1.4 of **5y** in 88% yield. (see SI data of **5y**). Notably, the structure of **5f** and **5p** were confirmed unambiguously by single crystal X-ray analysis (Fig. 7).

2.4. Application in the gram scale and one-pot synthesis

For the practical utility of the present methodology, the scalability of the reaction was investigated. A gram-scale reaction using model substrates **3a** and **4a** was carried out and it gave the corresponding polycyclic triazole **5a** in good yield (88%) without attenuation of the yield of pilot-scale reaction (Scheme 2a). Importantly, the synthesized triazole **5a** was derivatized through alkylation reaction in 75% yield. Then, a one-pot reaction through in-situ generation of triazole **3a** via click reaction was investigated. After com-

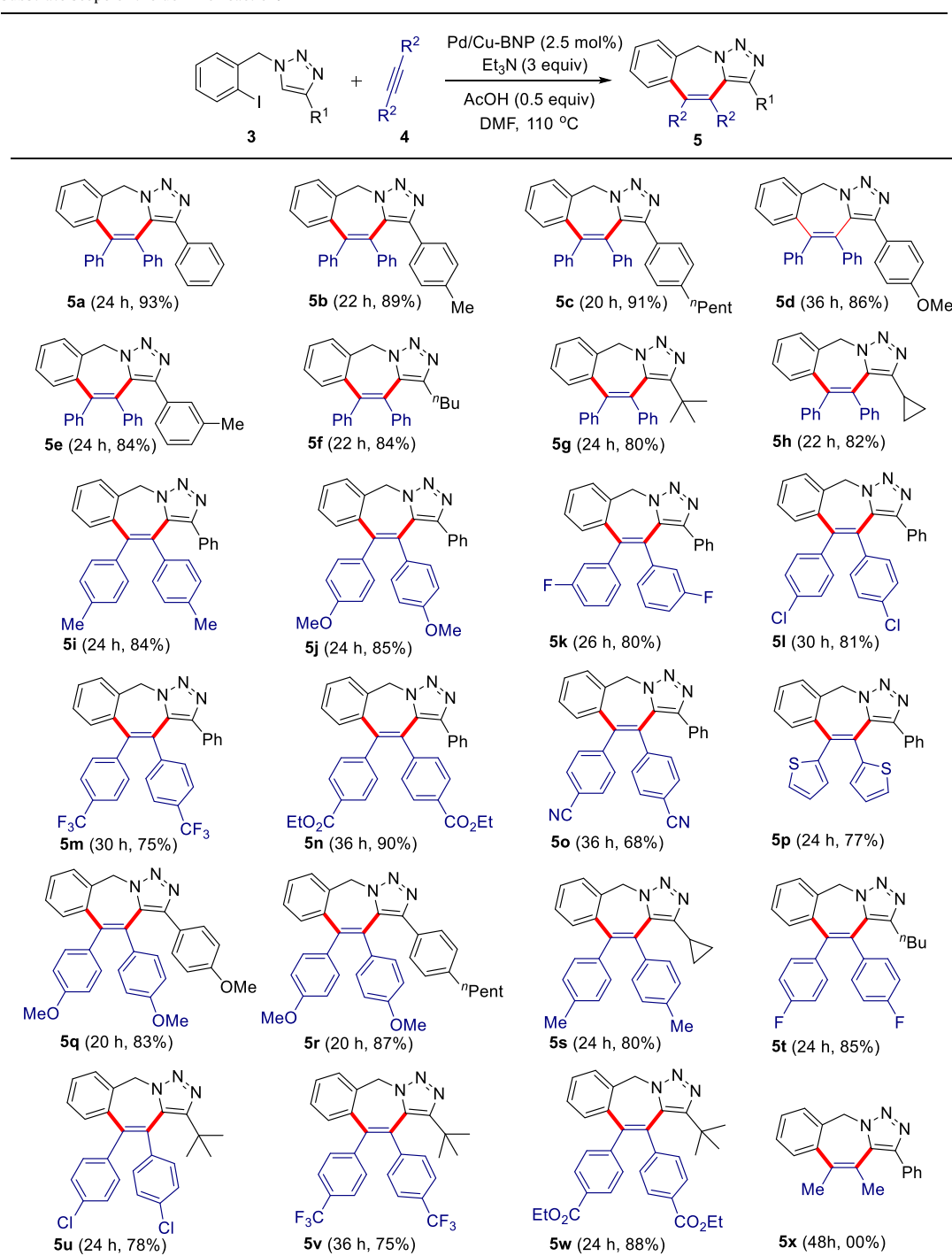
plete conversion of **7**, the Pd/Cu-BNP and **4a** were added to afford the annulated product **5a** in 61% yield (Scheme 2b). The one-pot reaction through in-situ generation of both the coupling partners also yielded the desired product in 48% yield highlighting the practicability of the current methodology (Scheme 2c).

2.5. Investigation of catalyst stability in reaction medium

Further efforts were made to examine the recoverability and reusability of the Pd/Cu-BNP catalyst. The model reaction was conducted at 1 mmol scale using triazole **3a** with **4a** under the optimized reaction conditions. The catalyst was recovered and reused up to 4 catalytic cycles and desired product **5a** was isolated in the yields of 92%, 90%, 87% and 86% in successive runs which proved the preserved activity of the catalyst (Fig. 8). To confirm that the reaction is catalyzed by heterogeneous Pd/Cu-BNP and not by the leached homogeneous Pd/Cu, the heterogeneous test such as hot centrifugation test and mercury poisoning test were conducted. In hot centrifugation test, the Pd/Cu-BNP was removed from reaction mixture by centrifuging in the middle of the reaction at two different time intervals from two different set of reactions. After that, both the filtrates (liquid portions) were allowed to continue stir at 110 °C. It was observed that the reaction did not proceed in both the liquid portions. It is clear that active species is Pd/Cu-BNP and not the leached out Pd or Cu atoms (Fig. 8).

HRTEM image of fresh catalyst and reused catalyst showed that particles size are similar which confirmed that the synthesized Pd/Cu-BNPs is stable in reaction medium (Fig. 9). Also, it was further confirmed from mercury poisoning test that the reaction is catalyzed by heterogeneous Pd/Cu nanocatalyst, not by leaching of homogeneous Pd/Cu.

Table 3
Substrate scope of the domino reaction.^a



^a All the reactions were carried out on 0.25 mmol scale and isolated yields are shown.

2.6. Preliminary investigations of reaction mechanism

Based on the literature precedent [34], we propose the following mechanism as shown in Scheme 3. Initially, an oxidative addition occurs between Pd/Cu-BNP and triazole bearing aryl iodide **3** to give the intermediate **A** and subsequent migratory insertion of diarylacetylene produces the intermediate **B**. Next, an in-situ gen-

erated carboxylate anion from the reaction of AcOH with Et₃N undergoes a ligand exchange with iodide to give the intermediate **C**. Then, carboxylate ligand-assisted C–H bond activation occurs via concerted metallation deprotonation (CMD) process [43] to give the intermediate **E** which upon reductive elimination expels the desired product **5** with a regeneration of active catalytic species for the next catalytic cycle.

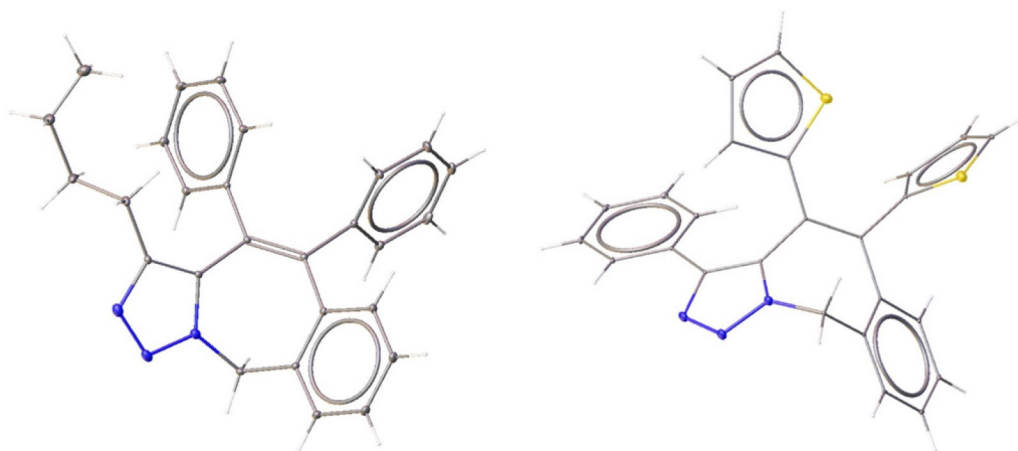
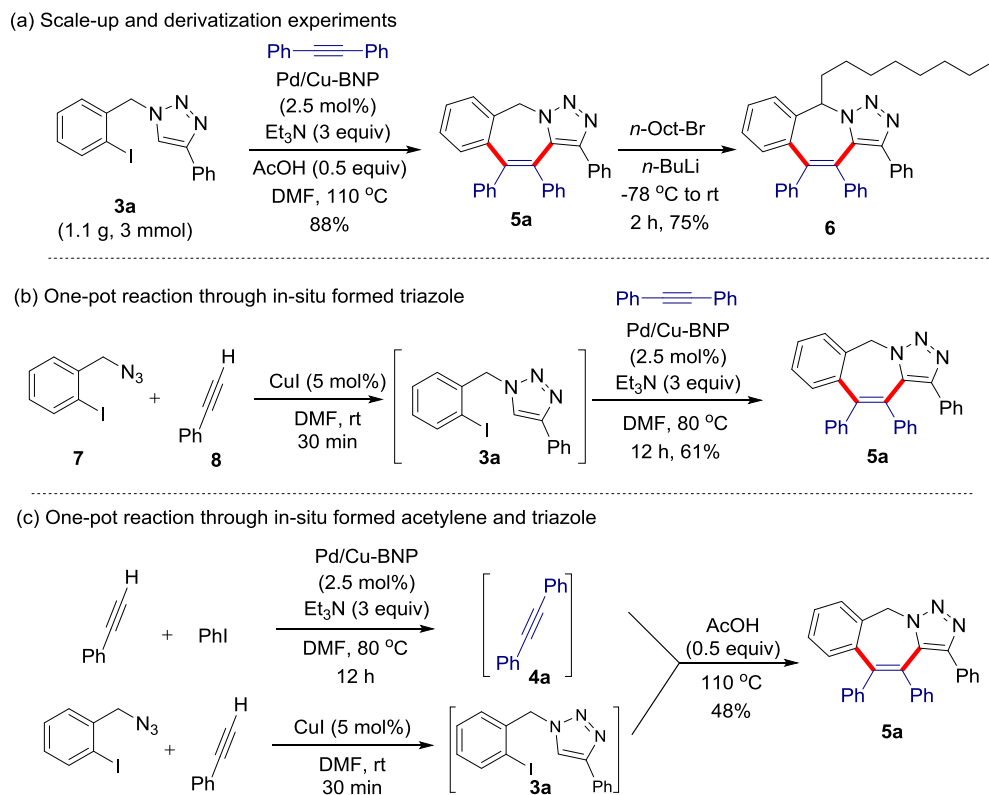


Fig. 7. ORTEP diagram of **5f** (left) and **5p** (right). The thermal ellipsoids are shown at 50% probability level (CCDC: 1852522 and 1936036).



Scheme 2. Experiments to investigate the practicability of the Pd/Cu-BNP catalyzed domino reaction.

3. Conclusion

In conclusion, we have successfully synthesized metal-carbon covalent bond stabilized Pd/Cu bimetallic nanoparticles for the first time using simple binaphthyl moiety as stabilizers. The synthesized Pd/Cu-BNP was characterized by various physical methods and the surface enrichment of Pd atoms in the Pd/Cu-BNP with a narrow size distribution was observed. The XPS analysis confirmed that the synthesized Pd/Cu-BNPs contain the electron deficient Pd centre and electron rich Cu centre. Moreover, this newly developed electron deficient Pd nanomaterial shown excellent catalytic activity for the synthesis of polycyclic triazoles via domino carbopalladation and C(sp²)-H bond functionalization

sequence. In addition, the catalyst has shown recyclability and was also found to be heterogeneous in nature. However, a detailed mechanistic study, biological activity of synthesized tricyclic triazoles and efforts to make chiral bimetallic nanoparticles are currently underway in our laboratory.

4. Methods

4.1. General procedure for Pd/Cu-BNP catalyzed synthesis of polycyclic triazoles

Under the open atmosphere, 1,2,3-triazole **3** (0.25 mmol), diaryl acetylene **4** (1.5 equiv.), 2.5 mol% of Pd/Cu-BNP (10 wt% Pd and

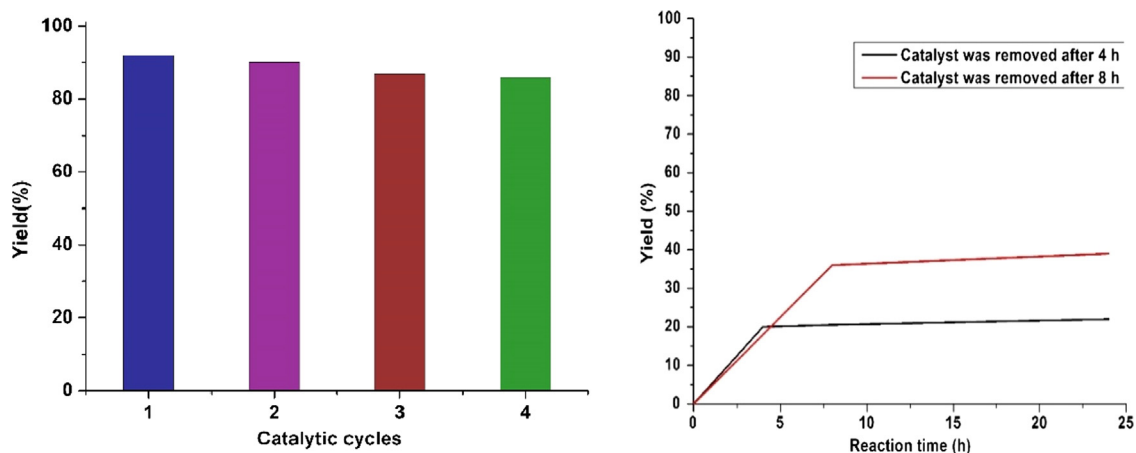


Fig. 8. Recyclability of the Pd/Cu-BNP (left) and Hot-filtration test (right).

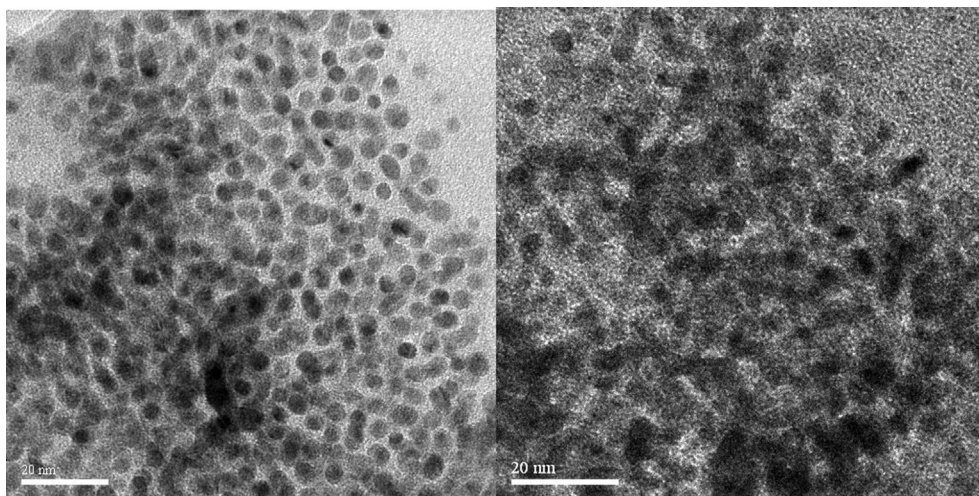
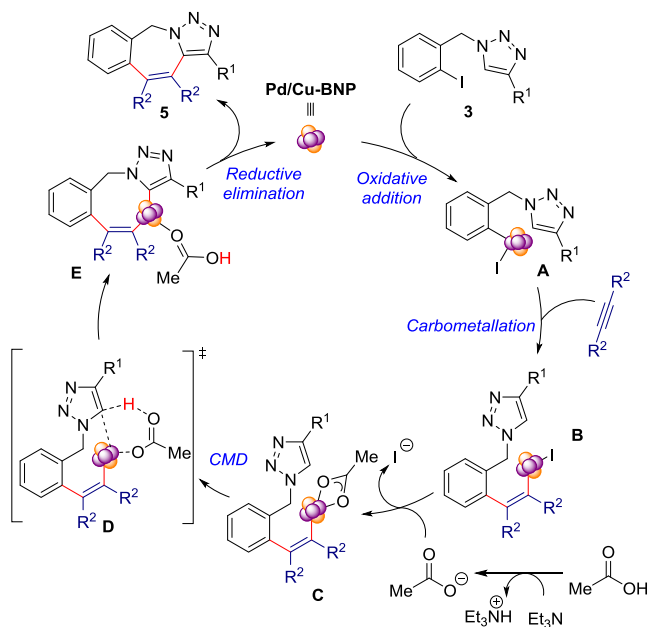


Fig. 9. HRTEM image of fresh (left) and reused (right) Pd/Cu-BNP.



Scheme 3. Proposed catalytic pathway.

5 wt% Cu by ICP-OES analysis) and DMF (1.5 mL) were successively added to oven dried reaction tube. Then Et_3N (1.5 mmol) and AcOH (50 mol%) were added and closed with a glass-stopper. The reaction tube was then immersed in pre-heated oil bath with magnetic pellet and stirred at 110°C . The reaction was heated with stirring till complete consumption **3**. After cooling down to room temperature, the solvent was removed under reduced pressure. Water was added to the reaction mixture and extracted with ethyl acetate (3×5 mL). Brine wash (1×10 mL) was given to the combined organic extractions and dried over anhydrous Na_2SO_4 . Removal of solvent and silica gel column separation of crude using hexanes and ethyl acetate mixture (4:1) afforded the corresponding tri-cyclic triazoles **5a-w**.

Acknowledgements

G.S thanks IIT Madras for exploratory research project (CHY/16-17/846/RFER/GSEK). R.S thanks IIT Madras for senior research fellowship and D.A thanks CSIR, New Delhi for senior-SPM fellowship. We thanks to Prof. T. Pradeep for XPS and HRTEM analysis. We would like to thanks department of metallurgical and materials engineering at IIT Madras for STEM analysis.

Appendix A. Supplementary material

Supplementary data to this article can be found online at <https://doi.org/10.1016/j.jcat.2019.07.063>.

References

- [1] D. Astruc, Ed. *Nanoparticles and Catalysis*, Wiley-VCH Verlag GmbH & Co. KGaA, 2008.
- [2] L.L. Chng, N. Erathodiyil, J.Y. Ying, Nanostructured catalysts for organic transformations, *Acc. Chem. Res.* 46 (2013) 1825–1837.
- [3] D. Ganapathy, G. Sekar, Palladium nanoparticles stabilized by metal-carbon covalent bond: An efficient and reusable nanocatalyst in cross-coupling reactions, *Catal. Commun.* 39 (2013) 50–54.
- [4] R. Saha, G. Sekar, Stable Pd-nanoparticles catalyzed domino C-H activation/C-N bond formation strategy: An access to phenanthridinones, *J. Catal.* 366 (2018) 176–188.
- [5] D. Ganapathy, G. Sekar, Efficient synthesis of polysubstituted olefins using stable palladium nanocatalyst: applications in synthesis of tamoxifen and isocombretastatin A4, *Org. Lett.* 16 (2014) 3856–3859.
- [6] R. Saha, N. Perveen, N. Nihesh, G. Sekar, Reusable palladium nanoparticles catalyzed oxime ether directed ortho-hydroxylation under phosphine free neutral condition, *Adv. Synth. Catal.* 361 (2019) 510–519.
- [7] N. Parveen, R. Saha, G. Sekar, Stable and reusable palladium nanoparticles-catalyzed conjugate addition of aryl iodides to Enones: route to reductive heck products, *Adv. Synth. Catal.* 359 (2017) 3741–3751.
- [8] R. Saha, D. Arunprasad, G. Sekar, Phosphine-free and reusable palladium nanoparticles-catalyzed domino strategy: synthesis of indanone derivatives, *J. Org. Chem.* 83 (2018) 4692–4702.
- [9] X. Liu, X. Wen, R. Hoffmann, Surface activation of transition metal nanoparticles for heterogeneous catalysis: what we can learn from molecular dynamics, *ACS Catal.* 8 (2018) 3365–3375.
- [10] N. Toshima, T. Yonezawa, Bimetallic nanoparticles - novel materials for chemical and physical applications, *New J. Chem.* 22 (1998) 1179–1201.
- [11] F. Tao, Synthesis, catalysis, surface chemistry and structure of bimetallic nanocatalysts, *Chem. Soc. Rev.* 41 (2012) 7977–7979.
- [12] J. Mao, Y. Liu, Z. Chen, D. Wang, Y. Li, Bimetallic Pd-Cu nanocrystals and their tunable catalytic properties, *Chem. Commun.* 50 (2014) 4588–4591.
- [13] R.K. Rai, D. Tyagi, K. Gupta, S.K. Singh, Activated nanostructured bimetallic catalysts for C-C coupling reactions: recent progress, *Catal. Sci. Technol.* 6 (2016) 3341–3361.
- [14] D. Kim, J. Resasco, Y. Yu, A.M. Asiri, P. Yang, Synergistic geometric and electronic effects for electrochemical reduction of carbon dioxide using gold-copper bimetallic nanoparticles, *Nat. Commun.* 5 (2014) 4948.
- [15] G.C.Y. Choo, H. Miyamura, S. Kobayashi, Synergistic cascade catalysis by metal nanoparticles and Lewis acids in hydrogen autotransfer, *Chem. Sci.* 6 (2015) 1719–1727.
- [16] F. Tao, S. Zhang, L. Nguyen, X. Zhang, Action of bimetallic nanocatalysts under reaction conditions and during catalysis: evolution of chemistry from high vacuum conditions to reaction conditions, *Chem. Soc. Rev.* 41 (2012) 7980–7993.
- [17] T. Yasukawa, H. Miyamura, S. Kobayashi, Polymer-incarcerated chiral Rh/Ag nanoparticles for asymmetric 1,4-addition reactions of arylboronic acids to enones: remarkable effects of bimetallic structure on activity and metal leaching, *J. Am. Chem. Soc.* 134 (2012) 16963–16966.
- [18] Z. Zhang, Y. Wang, X. Wang, Nanoporous bimetallic Pt-Au alloy nanocomposites with superior catalytic activity towards electro-oxidation of methanol and formic acid, *Nanoscale* 3 (2011) 1663–1674.
- [19] G.-H. Wang, J. Hilgert, F.H. Richter, F. Wang, H.-J. Bongard, B. Spliethoff, C. Weidenthaler, F. Schueth, Platinum-cobalt bimetallic nanoparticles in hollow carbon nanospheres for hydrogenolysis of 5-hydroxymethylfurfural, *Nat. Mater.* 13 (2014) 293–300.
- [20] C. Morabito, S. Guarnieri, A. Catizone, C. Schiraldi, G. Ricci, M.A. Mariggio, Transient increases in intracellular calcium and reactive oxygen species levels in TCam-2 cells exposed to microgravity, *Sci. Rep.* 7 (2017) 1–11.
- [21] C. Plana, S. Armenise, A. Monzon, E. Garcia-Bordeje, Ni on alumina-coated cordierite monoliths for in situ generation of CO-free H₂ from ammonia, *J. Catal.* 275 (2010) 228–235.
- [22] M.B. Gawande, A. Goswami, T. Asefa, H. Guo, A.V. Biradar, D.-L. Peng, R. Zboril, R.S. Varma, Core-shell nanoparticles: synthesis and applications in catalysis and electrocatalysis, *Chem. Soc. Rev.* 44 (2015) 7540–7590.
- [23] A. Wong, Q. Liu, S. Griffin, A. Nicholls, J.R. Regalbuto, Synthesis of ultrasmall, homogeneously alloyed, bimetallic nanoparticles on silica supports, *Science* 358 (2017) 1427–1430.
- [24] D. Chen, P. Sun, H. Liu, J. Yang, Bimetallic Cu-Pd alloy multipods and their highly electrocatalytic performance for formic acid oxidation and oxygen reduction, *J. Mater. Chem. A* 5 (2017) 4421–4429.
- [25] S. Guo, X. Zhang, W. Zhu, K. He, D. Su, A. Mendoza-Garcia, S.F. Ho, G. Lu, S. Sun, Nanocatalyst superior to Pt for oxygen reduction reactions: the case of core/shell Ag(Au)/CuPd nanoparticles, *J. Am. Chem. Soc.* 136 (2014) 15026–15033.
- [26] I. Nakamura, Y. Yamanoi, T. Imaoka, K. Yamamoto, H. Nishihara, A uniform bimetallic rhodium/iron nanoparticle catalyst for the hydrogenation of olefins and nitroarenes, *Angew. Chem., Int. Ed.* 50 (2011) 5830–5833, 5830/5831–5830/5835.
- [27] F. Mirkhalaf, J. Paprotny, D.J. Schiffrin, Synthesis of metal nanoparticles stabilized by metal-carbon bonds, *J. Am. Chem. Soc.* 128 (2006) 7400–7401.
- [28] A. Lauria, R. Delisi, F. Mingoia, A. Terenzi, A. Martorana, G. Barone, A.M. Almerico, 1,2,3-Triazole in heterocyclic compounds, endowed with biological activity, through 1,3-dipolar cycloadditions, *Eur. J. Org. Chem.* 2014 (2014) 3289–3306.
- [29] R. Li, D.J. Jansen, A. Datta, Intramolecular azide-alkyne [3 + 2] cycloaddition: versatile route to new heterocyclic structural scaffolds, *Org. Biomol. Chem.* 7 (2009) 1921–1930.
- [30] G. Biagi, I. Giorgi, O. Livi, V. Scartoni, L. Betti, G. Giannaccini, M.L. Trincavelli, New 1,2,3-triazolo[1,5-a]quinoxalines: synthesis and binding to benzodiazepine and adenosine receptors. II, *Eur. J. Med. Chem.* 37 (2002) 565–571.
- [31] R. Kharb, P.C. Sharma, M.S. Yar, Pharmacological significance of triazole scaffold, *J. Enzyme Inhib. Med. Chem.* 26 (2011) 1–21.
- [32] J.M. Schulman, A.A. Friedman, J. Pantelev, M. Lautens, Synthesis of 1,2,3-triazole-fused heterocycles via Pd-catalyzed cyclization of 5-iodotriazoles, *Chem. Commun.* 48 (2012) 55–57.
- [33] J.R. Donald, S.F. Martin, Synthesis and diversification of 1,2,3-triazole-fused 1,4-benzodiazepine scaffolds, *Org. Lett.* 13 (2011) 852–855.
- [34] Z. Qureshi, J.Y. Kim, T. Bruun, H. Lam, M. Lautens, Cu/Pd-catalyzed synthesis of fully decorated polycyclic triazoles: Introducing C-H functionalization to multicomponent multicatalytic reactions ((MC)2R), *ACS Catal.* 6 (2016) 4946–4952.
- [35] D. Ghosh, S. Chen, Palladium nanoparticles passivated by metal-carbon covalent linkages. [Erratum to document cited in CA148:437935], *J. Mater. Chem.* 19 (2009) 9287.
- [36] H. Masai, K. Sonogashira, N. Hagihara, The infrared spectra of the square-planar dialkyl complexes of nickel(II), palladium(II) and platinum(II), *J. Organomet. Chem.* 26 (1971) 271–276.
- [37] C.J. Corcoran, H. Tavassol, M.A. Rigsby, P.S. Bagus, A. Wieckowski, Application of XPS to study electrocatalysts for fuel cells, *J. Power Sources* 195 (2010) 7856–7879.
- [38] M. Wakisaka, S. Mitsui, Y. Hirose, K. Kawashima, H. Uchida, M. Watanabe, Electronic Structures of Pt-Co and Pt-Ru Alloys for CO-Tolerant Anode Catalysts in Polymer Electrolyte Fuel Cells Studied by EC-XPS, *J. Phys. Chem. B* 110 (2006) 23489–23496.
- [39] C.Q. Sun, Y. Wang, Y.G. Nie, B.R. Mehta, M. Khanuja, S.M. Shivaprasad, Y. Sun, J. S. Pan, L.K. Pan, Z. Sun, Interface quantum trap depression and charge polarization in the CuPd and AgPd bimetallic alloy catalysts, *Phys. Chem. Chem. Phys.* 12 (2010) 3131–3135.
- [40] Z.D. Pozun, S.E. Rodenbusch, E. Keller, K. Tran, W. Tang, K.J. Stevenson, G. Henkelman, A Systematic Investigation of p-Nitrophenol Reduction by Bimetallic Dendrimer Encapsulated Nanoparticles, *J. Phys. Chem. C* 117 (2013) 7598–7604.
- [41] E. Kim, H.S. Jeong, B.M. Kim, Efficient chemoselective reduction of nitro compounds and olefins using Pd-Pt bimetallic nanoparticles on functionalized multi-wall-carbon nanotubes, *Catal. Commun.* 45 (2014) 25–29.
- [42] H. Miyamura, A. Suzuki, T. Yasukawa, S. Kobayashi, Polysilane-immobilized Rh-Pt bimetallic nanoparticles as powerful arene hydrogenation catalysts: synthesis, reactions under batch and flow conditions and reaction mechanism, *J. Am. Chem. Soc.* 140 (2018) 11325–11334.
- [43] L. Ackermann, Carboxylate-assisted transition-metal-catalyzed C-H bond functionalizations: mechanism and scope, *Chem. Rev.* 111 (2011) 1315–1345.